Surface Review and Letters, Vol. 6, No. 6 (1999) 1061–1065

STRUCTURE DETERMINATION OF THE Ge(111)-(3 × 1)Ag SURFACE RECONSTRUCTION

D. GROZEA,* E. BENGU, C. COLLAZO-DAVILA and L. D. MARKS
Northwestern University, Department of Materials Science and Engineering, 2225 N. Campus Dr., room 2036 MLSB, Evanston, IL 60208, USA

Received 12 September 1999

For the first time, during the investigation of the Ag submonolayer on the Ge(111) system, large, independent domains of the Ge(111)-(3 × 1)Ag phase were imaged and investigated. Previous studies have reported it only as small insets between Ge(111)-(4 × 4)Ag and Ge(111)-c(2 × 8) domains. The transmission electron diffraction data were analyzed using a Direct Methods approach and "heavy-atom holography," with the result of an atomic model of the structure similar to that of Si(111)-(3 × 1)Ag.

1. Introduction

The formation of metallic overlayers on elemental semiconductor surfaces is of continuing scientific and technological interest. The (3 × 1) reconstruction, a low-coverage metal-induced structure, has been the subject of extensive investigations in the last decade. One of the reasons is its unusual chemical and electronic properties; for example, its presence induces passivation with respect to surface oxidation,1 and it has an unexpectedly large surface band gap.[2–4] It is induced by alkali metals and Ag on Si(111)[5,6] and Ge(111)[7,8] surfaces.

Another interesting characteristic of the (3 × 1) structure is the mounting evidence for only one common atomic structure regardless of the identity of the adsorbate. Low-energy electron diffraction (LEED) *I–V* curves have been shown to be almost identical for all the alkali metal reconstructions on Ge(111)[7] surfaces and, respectively, for alkali metal and Ag (3 × 1) reconstructions induced on Si(111)[9] surfaces. The scanning tunneling microscopy (STM) images of the (3 × 1) structure on Si(111) and Ge(111) are also similar; they show a cm symmetry plane group with a slight break of the mirror plane in the case of Ag-induced reconstruction.[2,4,8,10–12] The similarities extend to angle-resolved photoemission spectroscopy (ARPES) measurements, surface state bond dispersions[13–15] and surface core level shift (SCLS) spectra.[13,16]

While being able to account for some of the experimental data, none of the various structure models were consistent with all of the experimental observations.[13] The solution to the (3 × 1) atomic geometry was determined by Collazo-Davila, Grozea and Marks,[17] by applying Direct Methods to transmission electron diffraction (TED) data for Si(111)-(3 × 1)Ag; Fig. 1. Further extensive confirmation of this model came from theoretical studies by Erwin and Weitering[18] [who appropriately named it "honeycomb chain-channel" (HCC)] and Kang *et al.*[19] which showed this model to be by far more stable than any other models, from total-energy calculations from first principles.

Although the Ag/Si(111) interface has received considerable attention, the Ag/Ge(111) system has not been investigated as widely. Despite the similarities between the systems, there are major differences, especially in the lower-coverage Ag reconstructions.[6] In the Ag/Ge(111) system, a (4 × 4) structure forms prior to the $(\sqrt{3} \times \sqrt{3})$R30°. The Ag/Si(111) system forms a (3 × 1) structure which had never been observed on the Ge(111) surface over any extended areas. The Ge (3 × 1) has only been reported as

*Corresponding author. E-mail: dgrozea@merle.acns.nwu.edu

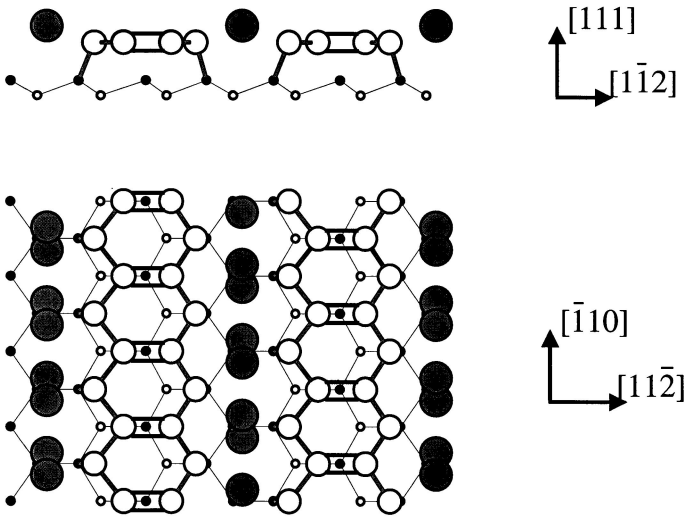

Fig. 1. Honeycomb chain-channel model. The gray circles represent the two equivalent half-occupied Ag sites and all other circles are semiconductor atoms.

narrow strips on the edge of (4×4) large domains from STM images.[4,8] The filled and empty states STM images were very similar to those of Si(111)-(3×1)Ag.[4,8]

In this paper, we report the observation for the first time of large domains of the (3×1) Ag-induced reconstruction in the Ag/Ge(111) system. Thermal treatments of the Ge(111)-(4×4)Ag phase induce its separation into a surface covered with $(\sqrt{3} \times \sqrt{3})$R30° and (3×1) domains. The Ag/Ge(111) system was investigated using TED and dark field images, with the result of an atomic model of the (3×1) structure similar to that of Si(111)-(3×1)Ag, the HCC model.

2. Experimental Procedure

Standard transmission electron microscopy (TEM) samples were prepared from Ge(111) wafers and introduced into SPEAR, an ultrahigh vacuum (UHV) surface preparation and analysis system attached to a high-resolution UHV H-9000 Hitachi transmission electron microscope.[20] Surface characteristics were monitored with X-ray photoelectron spectroscopy (XPS) and off-zone TED.

The samples were cleaned through cycles of ion milling and electron beam annealing until good TED patterns with clearly visible 1/2 order spots of the c(2×8) native reconstruction were obtained. After Ag deposition *in situ* at room temperature, reconstructions were induced on the surface using low temperature annealing. Ag coverage was estimated utilizing the relative Ag and Ge 3d XPS peak intensities.

The TEM images were collected at room temperature using an electron beam voltage of 200 kV to limit beam damage effects. The electron diffraction data set was obtained from a through-exposure series of nine diffraction patterns. After the negatives were digitized using an Optronics P1000 microdensitometer, the beam intensities were measured, reduced through a cross-correlation technique,[21] and averaged with the result of a final data set with estimated measurement errors.

3. Results and Discussion

After Ag deposition at room temperature on the Ge(111)-c(2×8) surface and a 350°C anneal of the specimen for a few minutes, TED patterns displayed the (4×4) reconstruction. Dark field images, Fig. 2(a), show triangular large domains of the (4×4) phase, and its corresponding (4×4) diffraction pattern is displayed in Fig. 2(b). On some of the edges of the triangular (4×4) domains, one or two linear features can be observed. They belong to the (3×1) structure, present only as narrow strips similar to STM data reports. Repeated annealing of this surface, again at 350°C for a few minutes, produced the

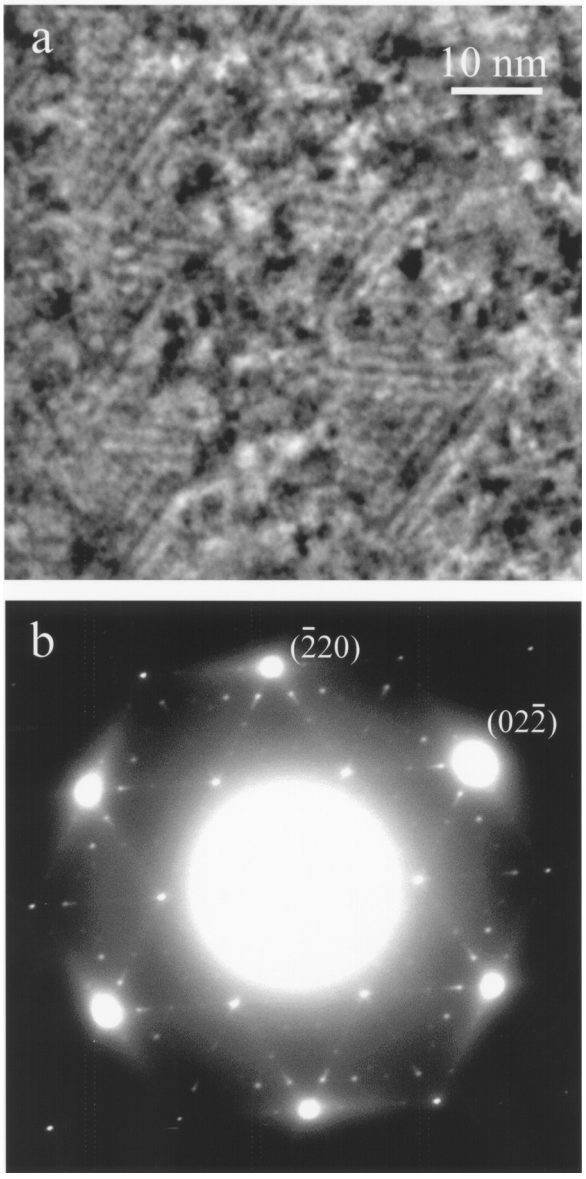

Fig. 2. (a) Dark field image of the (4×4) triangular domains with narrow strips of (3×1) structure visible on the edge as one or two linear features, and (b) corresponding (4×4) diffraction pattern.

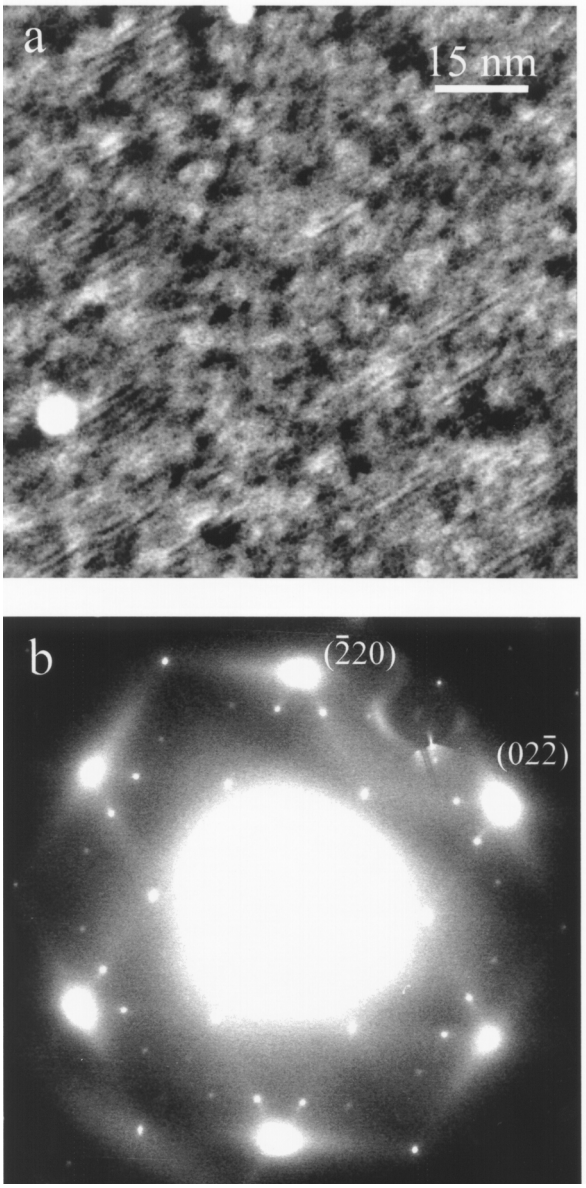

Fig. 3. (a) Dark field image showing linear features due to one domain of the (3×1) structure, and (b) corresponding diffraction pattern displaying both (3×1) and $(\sqrt{3} \times \sqrt{3})$ phases.

transformation of the (4×4) phase into large, independent (3×1) domains and $(\sqrt{3}\times\sqrt{3})$R30° regions. Dark field images, Fig. 3(a), show the complete disappearance of the (4×4) phase and the presence of (3×1) domains. No triangular (4×4) domains can be observed anymore, and only linear features due to the (3×1) phase are visible throughout the figure. The TED pattern, Fig. 3(b), exhibits both (3×1) and $(\sqrt{3} \times \sqrt{3})$ phases.

Direct Methods were applied to the diffraction data to find an initial model from which to refine atomic positions. X-ray or electron diffraction techniques provide only the intensities and not the phases of the beams. However, both intensity and phase are necessary to restore the charge density or the scattering potential, respectively. Direct Methods solve the phase problem by exploiting the probability

relationships which exist between the amplitudes and phases of the diffracted beams.[22] The method involves a routine search of sets of phase estimates for the measured beam intensities which best satisfy the probability relationships. The feasible solutions are defined by some figure of merit, and are in the form of potential maps generated using measured beam intensities and plausible sets of phases that satisfy self-consistent conditions.

However, the missing information that often characterizes surface diffraction data sets will induce artifacts and distorsions of the features present in the maps and preclude the interpretation of all bright circular features as atom sites.[23] Therefore, the maps are used only as a base to construct initial models of the investigated atomic structure. Figure 4 shows a contour map of the calculated surface scattering potential; all other solutions were practically the same.

Several models were constructed using the scattering potential map by combining iterative steps of minor refinement of the atomic positions (R-factor type) with "heavy-atom holography."[24] At the end of this analysis, an HCC model similar to the solution for the Si(111)-(3×1) reconstruction proved to be the best model, with a quick drop to the lowest value of R and no suggestion of new strong peaks by the maps. Other models based on different arrangements of Ge atoms and using full occupancy of Ag led to higher values of R and/or induced the algorithm to move the atoms to sites close to those of the Si(111) case.

As the next step, the atomic positions of the model were refined using a χ^2 minimization with full dynamical multislice calculations including the effects of bulk crystal diffraction and dynamical effects to arrive at the final structure. A reduced χ^2 value, defined as

$$\chi^2 \equiv \frac{1}{N-m} \sum_{j=1}^{N} \left(\frac{|I^j_{\text{expt}} - I^j_{\text{calc}}|}{\sigma_j} \right)^2 ,$$

where $I_{\text{expt}}/I_{\text{calc}}$ are the experimental/calculated beam intensities, σ is the error of the experimental intensity, N is the number of data points, and m is the number of parameters being fit, was calculated for the model while allowing one bulk double layer to relax. It gave a χ^2 value of 6.73. The number of variables (atomic positions, Debye–Waller factors for Ag and top surface Ge sites, and counting a scaling factor) was equal to 15 for 65 data points. To model the two equivalent Ag positions, where the Ag atom occupies an asymmetric location with respect to the $[\bar{1}10]$ direction, the occupancy factor for both locations was kept at 0.5. Keeping the same total number of variables and one relaxed bulk double layer, the calculations were repeated for the other models. The X-ray model, with the metal atom not breaking the *cm* symmetry, gave a χ^2 of 8.2, while the extended Pandey and Seiwatz models yielded values between 9.0 and 15.0.

More refinement of the model, letting a second bulk double layer relax, reduced χ^2 to 3.01, with the number of variables increased to 21. Adding the occupancy factor for Ag as an additional parameter, together with a variable Debye–Waller factor for the first relaxed bulk double layer, led to a χ^2 value of 2.51, with 23 variables. The Ag occupancy refined to 0.48, confirming the disordered placement of Ag in the two equivalent sites.

In addition to the three structural elements (adatoms, dimers and π-bonded chains) which are frequently encountered as "building blocks" of the Si and Ge reconstructions, Erwin and Weitering[18] proposed a new one, a true Si double bond (Fig. 1), to explain the very low energy of the HCC model for the Si(111)-(3×1) structures, despite the fact that double bonds are unknown in ordinary compounds of Si and Ge.

The similarity between the Ge(111)-(3×1)Ag and Si(111)-(3×1)Ag structures may lead to the conclusion that the unusual double bond is not limited to Si but can also be formed by Ge atoms. Moreover, this double bond could be significant in stabilizing other

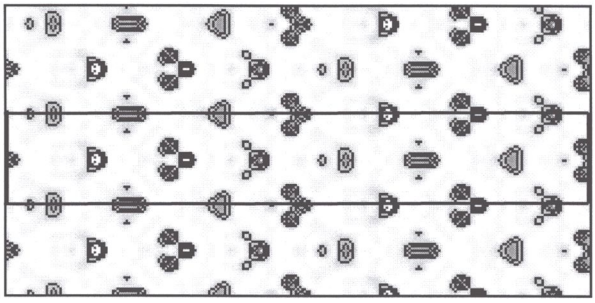

Fig. 4. Contour map of the calculated surface scattering potential using phases estimated through direct methods. In the center of the figure a (6×1) *cm* unit cell is outlined.

reconstructions. It has already been suggested[25] that the two structures are related and a double bond formation in this case also eliminates all the dangling bonds from the (4×4)'s Ge ring and contributes to its stability.

The (3×1) structure used to be considered not worth mentioning in the surface phase diagram of the Ag/Ge(111) system, since it was believed to not exist over any extended regions of the surface. This note clarifies the question of its existence and stability, and also provides a better understanding of the (4×4) reconstruction. This latter phase is metastable at room temperature and, after an appropriate thermal treatment, separates into (3×1) and $(\sqrt{3} \times \sqrt{3})$ domains.

Acknowledgment

This work was supported by the National Science Foundation under Grant #DMR-9214505.

References

1. M. Tikhov, L. Surnev and M. Kiskinova, *Phys. Rev.* **B44**, 3222 (1991).
2. D. Jeon, T. Hashizume, T. Sakurai and R. F. Willis, *Phys. Rev. Lett.* **69**, 1419 (1992).
3. J. M. Carpinelli and H. H. Weitering, *Phys. Rev.* **B53**, 12651 (1996).
4. H. H. Weitering and J. M. Carpinelli, *Surf. Sci.* **384**, 240 (1997).
5. H. Daimon and S. Ino, *Surf. Sci.* **164**, 320 (1985).
6. G. Le Lay, *Surf. Sci.* **132**, 169 (1983).
7. W. C. Fan and A. Ignatiev, *Phys. Rev.* **B40**, 5479 (1989).
8. M. Hammar, M. Göthelid, U. O. Karlsson and S. A. Flodström, *Phys. Rev.* **B47**, 15669 (1993).
9. W. C. Fan and A. Ignatiev, *Phys. Rev.* **B41**, 3592 (1990).
10. K. J. Wan, X. F. Lin and J. Nogami, *Phys. Rev.* **B46**, 13635 (1992).
11. T. Hashizume, M. Katayama, D.-R. Jeon, M. Aono and T. Sakurai, *Jpn. J. Appl. Phys.* **32**, L1263 (1993).
12. D. Jeon, T. Hashizume and T. Sakurai, *J. Phys.* IV, C5-189 (1996).
13. H. H. Weitering, X. Shi and S. C. Erwin, *Phys. Rev.* **B54**, 10585 (1996).
14. T. Okuda, K. Sakamoto, H. Nishimoto, H. Daimon, S. Suga, T. Kinoshita and A. Kakizaki, *Phys. Rev.* **B55**, 6762 (1997).
15. K. Sakamoto, T. Okuda, H. Nishimoto, H. Daimon, S. Suga, T. Kinoshita and A. Kakizaki, *Phys. Rev.* **B50**, 1725 (1994).
16. T. Okuda, H. Shigeoka, H. Daimon, S. Suga, T. Kinoshita and A. Kakizaki, *Surf. Sci.* **321**, 105 (1994).
17. C. Collazo-Davila, D. Grozea and L. D. Marks, *Phys. Rev. Lett.* **80**, 1678 (1998).
18. S. C. Erwin and H. H. Weitering, *Phys. Rev. Lett.* **81**, 2296 (1998).
19. M.-H. Kang, J.-H. Kang and S. Jeong, *Phys. Rev.* **B58**, R13359 (1998).
20. C. Collazo-Davila, E. Landree, D. Grozea, G. Jayaram, R. Plass, P. Stair and L. D. Marks, *J. Microsc. Soc. Am.* **1**, 267 (1995).
21. P. Xu, G. Jayaram and L. D. Marks, *Ultramicros.* **53**, 15 (1994).
22. M. M. Woolfson and H.-F. Fan, in *Physical and Non-Physical Methods of Solving Crystal Structures* (Cambridge University Press, Cambridge, 1995).
23. L. D. Marks, E. Bengu, C. Collazo-Davila, D. Grozea, E. Landree, C. Leslie and W. Sinkler, *Surf. Rev. Lett.* **5**, 1087 (1998).
24. D. Grozea, E. Landree, C. Collazo-Davila, E. Bengu, R. Plass and L. D. Marks, *Micron* **30**, 41 (1999).
25. C. Collazo-Davila, D. Grozea, L. D. Marks, R. Feidenhans'l, M. Nielsen, L. Seehofer, L. Lottermoser, G. Falkenberg, R. L. Johnson, M. Gothelid and U. Karlsson, *Surf. Sci.* **418**, 395 (1998).